Estimation of land subsidence caused by loss of smectite-interlayer water in shallow aquifer systems

Chen-Wuing Liu · Wen-Sheng Lin · Li-Hsin Cheng

Abstract Traditionally, land subsidence that results from groundwater over-pumping has often been described by the theory of consolidation. The mechanism of land subsidence due to the dehydration of clay minerals is not well addressed. A model of the "hydration state of smectite", and a "solid solution model of smectite dehydration", incorporating a thermodynamic solid solution model and laboratory results concerning clay-water systems of swelling pressure, hydration state and basal spacing in smectite interlayer, are employed to examine the effect of the release of water from the smectite interlayer on land subsidence in the coastal area of the Chou-Shui River alluvial fan and the Yun Lin offshore industrial infrastructure complex in Taiwan. The results indicate that 9.56–22.80% of the total cumulative land subsidence to a depth of 300 m is consistent with smectite dehydration following the over-pumping of groundwater. This dehydration-related land subsidence occurred to a depth of 0–60 m, with subsidence due to smectite dehydration accounting for 6.20–13.32% of the primary consolidation. Additionally, the total amount of subsidence resulting from both smectite dehydration and primary consolidation is consistent with the subsidence observed in the field. This study reveals that smectite dehydration appears to be important in assessing and predicting land subsidence in shallow aquifer systems.

Received: 30 January 2005 / Accepted: 25 March 2005
Published online: 24 November 2005

© Springer-Verlag 2005

C.-W. Liu (✉)
Department of Bioenvironmental Systems Engineering,
National Taiwan University,
Taipei, Taiwan, 10617 ROC
e-mail: lcw@gwater.agec.ntu.edu.tw
Tel.: +886-2-2362-6480
Fax: +886-2-2363-9557

W.-S. Lin
Water Resources Agency, Ministry of Economic Affairs,
Taipei, Taiwan, 106 ROC

L.-H. Cheng
Department of Industrial Safety and Hygiene, Foo-Yin University,
Kaohuing, Taiwan, 831 ROC

Résumé Traditionnellement la subsidence du terrain résultant d'une surexploitation des nappes est expliquée surtout par la théorie de la consolidation. On ne prend que rarement en compte la déhydratation des minéraux argileux comme mécanisme de la subsidence. Afin d'examiner l'effet de l'eau libérée par une couche de smectite sur la subsidence dans la zone côtière de l'aquifère alluvial de la rivière de Chou Shui ainsi que sur l'infrastructure du complexe offshore de Yu Lin on a utilisé un modèle " l'état de hydratations du smectite " et un modèle du "solution solide de déshydratation du smectite" qui considère aussi un modèle thermodynamique de la solution solide et des résultats des essais en laboratoire concernant la pression de gonflement dans le système eaux-argile, l'état de hydratation et l'écartement basale dans l'intercouche de smectite. Les résultats indiquent que de 9.56 à 22.80% de la subsidence cumulative jusqu' au profondeur de 300 m est compatible avec la déshydratation du smaltite qui a suivi le pompage excessif de l'aquifère. La subsidence liée au déshydratation se produise dans l'intervalle de profondeur de 0 à 60 m et rend compte de 6.20% à 13.32 de la consolidation primaire. De plus la subsidence totale qui résulte de la déshydratation du smectite et la consolidation primaire est en accord avec la valeur mesurée sur le terrain. L'étude met en évidence que la déshydratation du smaltite peut être un élément important dans léstimation et la prévision de la subsidence des aquifères de surface.

Resumen Tradicionalmente, la subsidencia del terreno que resulta de la explotación exagerada del agua subterránea, ha sido descrita a menudo por la teoría de consolidación. El mecanismo de subsidencia del terreno debido a la deshidratación de los minerales arcillosos no está bien enfocado. Se ha empleado un modelo del "estado de hidratación de la esmectita" y también de "disolución sólida de la deshidratación de la esmectita", incorporando un modelo termodinámico de disolución sólida y resultados de laboratorio relacionados con la presión de expansión en sistemas agua - arcilla, estado de hidratación y espaciamiento basal en las láminas de esmectita; todo lo anterior, con el fin de examinar el efecto de la liberación de agua en láminas de esmectita, sobre la subsidencia del terreno en el área costera del cono aluvial del río Chou - Shui y sobre la infraestructura del complejo industrial de Yun Lin, ubicado costa afuera en Taiwan. Los resultados indican que entre un

 DOI 10.1007/s10040-005-0459-0

9.56%–22.8% del total de la subsidencia acumulada porel terreno, hasta una profundidad de 300 m, esta coincidiendo con la deshidratación de la esmectita debida a sobre—explotación del agua subterránea. Esta subsidencia del terreno debida a deshidratación sucedió para profundidades entre 0–60 m, con una subsidencia debida a deshidratación de la esmectita, que oscila entre 6.20% al 13.32% de la consolidación primaria. Adicionalmente, la cantidad total de subsidencia que resulta tanto de la deshidratación de la esmectita, como de la consolidación primaria, está de acuerdo con la subsidencia observada en el campo. Este estudio revela que la deshidratación de la esmectita, parece ser importante en la evaluación y predicción de la subsidencia del terreno en sistemas acuíferos someros.

Keywords Thermodynamic model · Smectite dehydration · Subsidence · Shallow aquifer

Introduction

Land subsidence that results from over-pumping of groundwater proceeds by two main processes—primary consolidation and secondary compression. Primary consolidation is caused by the dissipation of excess pore water pressure, which gradually increases the effective stress on the soil skeleton. The amount of primary consolidation due to the increase of effective stress can be determined using Terzaghi's theory of consolidation (Terzaghi 1943). After the excess pore water pressure dissipates, secondary compression slowly and continuously develops, including slippage of soil particles, release of water from soil microfabric elements, expulsion of water from clay minerals and the surface interaction of the readjustment of the positions of the attached cations. Of these processes, the dehydration of smectite is an important part of secondary compression. The transient void ratio against the effective stress in the secondary compression indicates that as the effective stress is applied for long periods, the soil particles are compacted more densely (Mitchell 1993).

The effective stress drives the soil compaction by the processes of primary consolidation and secondary compression. As soil compaction begins, dissipation of excess pore pressure and the rearrangement of the soil structure may occur concurrently. The correct approach when evaluating soil compaction is to formulate the governing equations of the coupling processes and solve them analytically or numerically. Mitchell (1993) showed that the flow equation for the dynamic dissipation of excess pore water, the clay dehydration equation and the constitutive equation of soil/water rheology are difficult to develop and solve. Biot (1941, 1955) developed a three dimensional elastic model coupled with excess pore water pressure to evaluate primary consolidation. Bethke (1986) proposed a compaction model that considered various effects, including the release of water due to clay dehydration. However, Bethke's model did not incorporate Terzaghi's or Biot's principle of effective stress, and the mechanics of compaction were not addressed rigorously. Audet (1995) developed a one-dimensional model of the gravitational compaction of thick sediment layers in which the sediments undergo a thermally activated dehydration reaction of smectite to illite, releasing pore fluid at depth. Chemically released water can increase the excess pore pressure by as much as 30% for a relatively impermeable sediment. If sediments overlie a permeable base, then fluid can flow out of the sediments, relieving pore pressure throughout the sedimentary column.

In a shallow aquifer system, the over-pumping of groundwater may partially dehydrate the clay minerals; however, the transition of semectite to illite is unlikely to occur because of the small temperature effect. Liu et al. (2001) applied the semectite dehydration theory of Ransom and Helgeson (1994a, 1994b, 1995) to evaluate the effect of clay dehydration on the cumulative amount of land subsidence in the Yun Lin coastal area in Taiwan. However, they did not consider the nonlinear relationships between both the swelling pressure and the basal spacing and the ratio of the mass of water to the mass of smectite. The computed subsidence due to the smectite dehydration is overestimated.

This study aims is to apply a rigorous thermodynamic model of smectite dehydration for evaluating subsidence in a shallow sedimentary basin. An interlayer hydration state model and a solid solution model of interlayer dehydration are employed to account for the effect of dehydration of smectite on subsidence due to the over-pumping of groundwater in the coastal area of the Chou-Shui River alluvial fan and in the Yun Lin offshore industrial infrastructure complex in Taiwan (Fig. 1). The subsidence caused by smectite dehydration is quantified using in-situ stratigraphic data collected from the subsidence-monitoring wells in the field. The results of smectite dehydration are compared to the accumulated subsidence observed in the field. Furthermore, the amount of subsidence due to the complete dehydration of smectite is computed from the theoretical model and the possible mechanisms of subsidence that may occur in the shallow sedimentary basin are discussed.

Method and models

The isomorphic substitution of Al^{3+} and Mg^{2+} in smectite octahedral sites, or of Si^{4+} by Al^{3+} in smectite tetrahedral sites generates an excess negative charge on the smectite lattice. The excess negative lattice charge is compensated for by the adsorption of cations on the smectite sheets. In the presence of water, the compensating cations on smectite layers may easily be exchanged for other cations (such as Ca^{2+}, Mg^{2+}, Na^{+} or K^{+}) when they are available in solution. Moreover, the hydration of smectite will create a negative hydroxyl surface charge (such as in Si-OH or Al-OH). The polar structure of water molecules is such that water is strongly adsorbed onto the surface of smectite. If the water is adsorbed by the interlayer of smectite, it is called interlayer water.

Colten-Bradley (1987) stated that the smectite interlayer includes four discontinuous basal spacings of ~10 Å, ~12 Å, ~15.5 Å and ~18.5 Å. The 10 Å basal spacing

 DOI 10.1007/s10040-005-0459-0

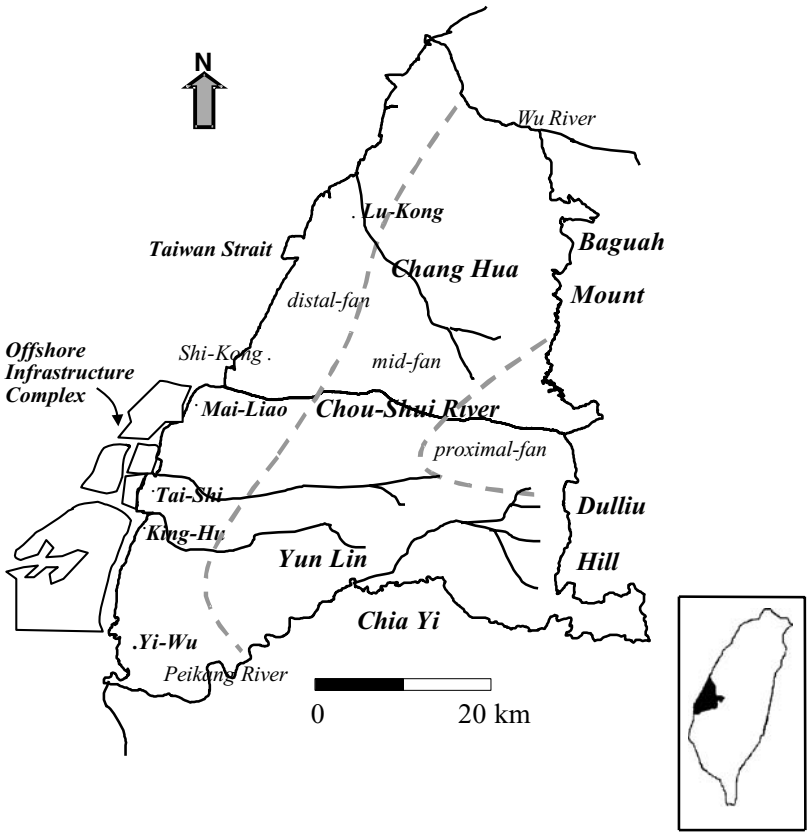

Fig. 1 Location of Chou-Shui River alluvial fan in Taiwan

is free from water molecules whereas the ~15.5 Å basal spacing contains 20 wt% water and the ~18.5 Å basal spacing contains 25 wt% water (Fitts and Brown 1999). The hydration state, or the amount of interlayer water, is a function of the extent and location of the 2:1 layer charge, the interlayer cation species, the vapor pressure, the temperature and the salinity of associated water (Keren and Shainberg 1975; Sato et al. 1992; Bray et al. 1998; Fitts and Brown 1999).

Applying the theory of thermodynamic solid solution of smectite (Ransom and Helgeson 1989, 1994a, 1994b, 1995), the laboratory results concerning clay-water system of swelling pressure and interlay water content (Oliphant and Low 1982; Zhang and Low 1989; Fu et al. 1990), and the concept of porosity corrections for smectite-rich sediment (Brown and Ransom 1996; Fitts and Brown 1999), a model of the "hydration state of smectite", and a "solid solution model of smectite dehydration" are employed to examine the effect of the release of water from the smectite interlayer on land subsidence in the coastal area of the Chou-Shui River alluvial fan and Yun-Lin offshore industrial infrastructure complex.

Relationship between release of interlayer water and land subsidence

The hydration condition of the layers of water molecules adsorbed on the smectite increases monotonically, from one in increments of one according to the increase in the wetness. Three driving forces govern the swelling of hydrated smectite, including the surface hydration force, the osmotic hydration force and the capillary force, the first two of which are more important than the last. Water molecules adsorbed onto the surface and into interlayer positions cause lattice swelling. At low humidity, only the surface adsorbs water molecules and exchangeable cations in the interlayer. It is also free from hydration. As the humidity increases, the exchangeable interlayer cations begin to hydrate and the interlayer spacing increases in a stepwise fashion. As the humidity further increases, the externally adsorbed water molecules become multiplayers and fill up exterior micro pores. The osmotic hydration force is generated by the chemical potential of the interlayer cations being higher than that of the free ions in bulk solution. As a result, water molecules diffuse into the interlayer region, increase the basal spacing and form a diffusive electrical double layer.

Zhang and Low (1989) experimentally determined the relationship between basal spacing and the ratio of the water mass (m_w) to the smectite mass (m_c) in the Na-smectite/water system. As the ratio m_w/m_c increases from 0.0 g/g to 4.5 g/g, the basal spacing increases from ~10 Å to ~110 Å. However, as m_w/m_c increases from 0.6 g/g to 1.0 g/g, basal spacings discontinuously jump from ~19 Å to 32 Å. The discontinuous jump may be caused by the increase in the number of exchangeable cations on the negatively charged smectite surface as the interlayer hydration spacing increases. If the expulsive forces of the interlayer cations exceed the van der Waal's forces, then

 DOI 10.1007/s10040-005-0459-0

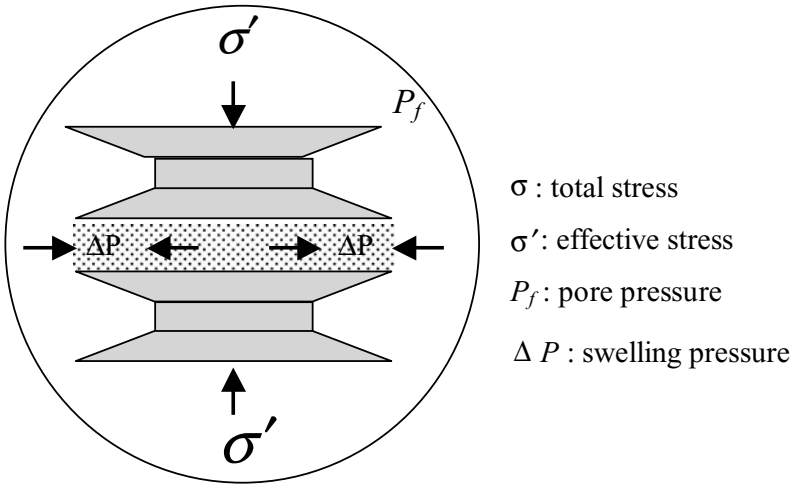

Fig. 2 Schematic diagram of the equilibrium between swelling pressure and effective stress in the interlayer of Na-smectite (after Fitts and Brown 1999)

the attractive forces on the negatively charged surface and the dipole attraction may trigger an unstable discontinuous jump. Oliphant and Low (1982) measured swelling pressure against the thermodynamic parameters of enthalpy and entropy in a smectite-water system and yielded a regression relationship between the change in swelling pressure and m_w/m_c. According to the experimental and interpolated data on swelling pressure over m_w/m_c (Oliphant and Low 1982) and the relationship between basal spacing and m_w/m_c (Zhang and Low 1989), Fig. 3 completely describes the relationships among m_w/m_c, basal spacing and the swelling pressure. The basal spacing decreases from 110 Å to 43 Å, and m_w/m_c reduces accordingly from ~4 g/g to 1.5 g/g. As the m_w/m_c decreases further, the swelling pressure drops quickly and even becomes negative. The substantial drop of swelling pressure, corresponding to the discontinuous jump is in the range of m_w/m_c from 0.6 g/g to 1.0 g/g.

Consider the equilibrium condition in which swelling pressure balances the effective stress in a Na-smectite system (Fig. 2). Based on the regression equation in Fig. 3; as m_w/m_c (the ratio of the water mass (m_w) to the smectite mass (m_c) in the Na-smectite/water system) decreases from ~5 g/g to ~1.5 g/g, the corresponding swelling pressure increases from 64.94 kPa (approximately 6 m below the land surface) to 740.95 kPa (approximately 66 m depth below the land surface) and then reaches a critical value P. If m_w/m_c further declines from ~1.5 g/g, then the swelling pressure will drop rapidly even to negative value, triggering a discontinuous jump in the basal spacing. Thus, the pumping of groundwater results in a drawdown of groundwater and decreases the pressure of the pore water. The effective stress applied to the hydrous smectite increases correspondingly. Based on Fig. 3, three different conditions may pertain.

1. *Condition 1*: The original effective stress applied to the smectite is under 740.95 kPa. As the groundwater is pumped, the effective stress increases but remains lower than 740.95 kPa. This condition is said to pertain Zone A, to the right hand of the critical point P (Fig. 3). In Zone A, the swelling pressure increases as m_w/m_c decreases and the basal spacing decreases accordingly.

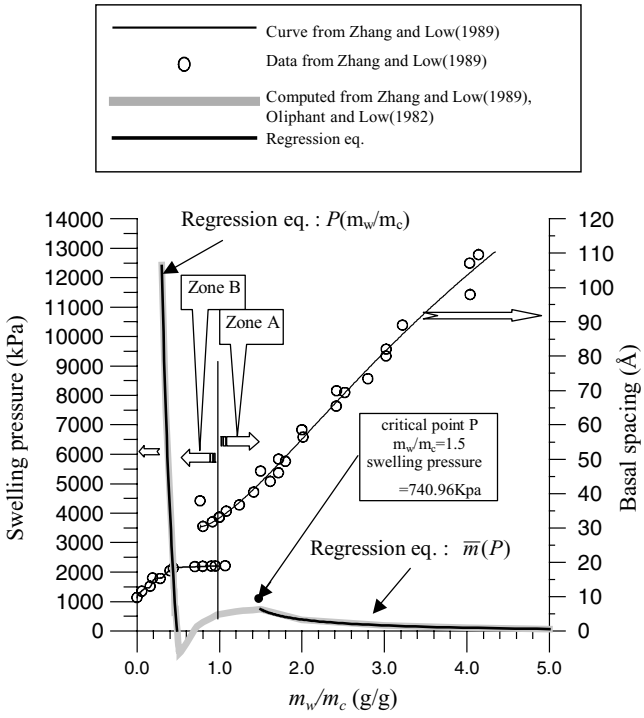

Fig. 3 Relationship among swelling pressure, basal spacing and m_w/m_c in a Na-smectite water system at 25°C

2. *Condition 2*: The original effective stress applied to the smectite is less than 740.95 kPa. As the groundwater is pumped, the effective stress increases and exceeds 740.95 kPa. The condition depicted in Fig. 3 reveals the original effective stress in Zone A, to the right hand of the critical point P, increases across the critical point P of a discontinuous jump in the basal spacing, and enters into Zone B. The basal spacing is reduced from its value under stable conditions to ~19 Å (m_w/m_c decreases to 1.0 g/g) and the dehydration reaction continues until it reaches chemical equilibrium.
3. *Condition 3*: The original effective stress applied to the smectite exceeds 740.95 kPa; that is, the smectite has to pass through the region of a discontinuous jump in the

 DOI 10.1007/s10040-005-0459-0

basal spacing and is in Zone B. The dehydration reaction is at chemical equilibrium. As the pumping begins, the increase in effective stress disturbs the dehydration reaction and leads to the dehydration reaction.

Given the above three dehydration conditions, two models for evaluating the effect of smectite dehydration on land subsidence due to the over pumping of groundwater are presented.

Subsidence due to the hydration state of the interlayer

Consider that the smectite is initially subjected to an effective stress below 740.95 kPa. The amount of subsidence of hydrous smectite is estimated from its interlayer's hydration state. Brown and Ransom (1996) and Fitts and Brown (1999) proposed a porosity (ϕ) modified equation for porosity based on the hydration state of smectite. The porosity of soil is defined as,

$$\phi \equiv \frac{V_v}{V_T} = \left(\frac{M_p}{\rho_w}\right) \Big/ \left(\frac{1}{\rho_b}\right) = \left(\frac{W_c M_s}{\rho_w}\right) \rho_b \tag{1}$$

where, ϕ: porosity, V_v: void volume of soil (cm^3), V_T: bulk volume of soil (cm^3), M_p: mass of water released by heating per unit mass of soil (g), M_s: mass of dry soil after dewatering by heating per unit mass of soil (g), W_c: ratio of per water mass to dry soil mass, ρ_w: pore water density (g/cm^3), ρ_b: soil bulk density (g/cm^3)

Additionally, $M_p + M_s = 1$, and $W_c = \frac{M_p}{M_s}$ leads to,

$$M_s = \frac{1}{1 + W_c} \tag{2}$$

Brown and Ransom (1996) noted that the preceding definition of porosity does not exclude the volume of interlayer water in the smectite. The interlayer water may be vaporized by heating such that the definition of smectite porosity in Eq. (1) may overestimate porosity. Brown and Ransom (1996) proposed to let α be the interlayer water mass per unit mass of smectite and A be the ratio of the heated dry smectite mass to the heated dry soil mass. The heated dry smectite mass is then $A/(1+W_c)$ and the mass of interlayer water of smectite (M_i) is,

$$M_i = \left(\frac{A}{1 + W_c}\right)\left(\frac{\alpha}{1 - \alpha}\right) \tag{3}$$

Thus, the modified water mass in the interlayer to the dry soil mass which, including the interlayer water mass, is,

$$\overline{W}_c = \frac{M_p - M_i}{M_s + M_i} = \frac{W_c(1 - \alpha) - A\alpha}{1 - \alpha + A\alpha} \tag{4}$$

Replacing $\overline{W}_c$ in Eqs. (1) and (2) with $\overline{W}_c$ in Eq. (4) yields the modified porosity equation of hydrous smectite,

$$\phi_\alpha = \frac{\rho_b}{\rho_w(1 + W_c)}\left(W_c - \frac{A\alpha}{1 - \alpha}\right) \tag{5}$$

and the relationship between W_c and ϕ is,

$$W_c = \frac{\phi \rho_w}{M_s \rho_b} \tag{6}$$

Thereby, the modified porosity equation of hydrous smectite can be expressed as,

$$\phi_\alpha = \frac{\rho_b\left(\frac{\phi\rho_w}{M_s\rho_b} - \frac{A\alpha}{1-\alpha}\right)}{\rho_w\left(1 + \frac{\phi\rho_w}{M_s\rho_b}\right)} \tag{7}$$

Regressing the equation for m_w/m_c the swelling pressure (P) for m_w/m_c from ~5 g/g to ~1.5 g/g in Fig. 3 yields,

$$\bar{m}(P) = a_4 + b_4/\ln P + c_4/(\ln P)^2 + d_4/(\ln P)^3 + e_4/(\ln P)^4 + f_4/(\ln P)^5 \tag{8}$$

where, $m \equiv m_w/m_c$, a_4=42.29, b_4=−813.70, c_4=5538.86, d_4=−14365.26, e_4=7932.78, f_4=14162.76

$$\alpha = \frac{\bar{m}(P)}{1 + \bar{m}(P)} \tag{9}$$

The value of α at different swelling pressures (or effective stress) can be determined using Eq. (8), and substituted in Eq. (6) to yield the modified porosity of smectite in the hydrous state. The physical interpretations of soil porosity (ϕ) and modified porosity of smectite in the hydrous state at α_1 and α_2 (where $\alpha_1 > \alpha_2$, $\phi > \phi_{\alpha_2} > \phi_{\alpha_1}$) are as follows.

The term ϕ is measured by vaporizing the interlayer water and thus overestimates the soil void volume and yields the largest porosity; a higher hydrous state of smectite refers to the occupancy of interlayer water of more void volume and a smaller porosity, and vice versa. Thus, the difference $\Delta\phi$ between the porosity in the hydrous states α_1 and α_2 of smectite is,

$$\Delta\phi = \phi_{\alpha_2} - \phi_{\alpha_1} \tag{10}$$

Initially, the aquifer is not over-pumped; the original hydrous state of smectite is at α_1. As the aquifer is over-pumped, the effective stress and the swelling pressure increase accordingly to compact the soil skeleton and expel water from the interlayer. The hydrous state of smectite is then α_2. The volume of water expelled from the interlayers of smectite in hydrous states α_1 and α_2 is $\Delta\phi \cdot V_T$ and equals the compressed volume of smectite. Accordingly, the amount of subsidence caused by the expulsion of interlayer water from smectite is,

$$H_1 = \Delta\phi \times d_c \tag{11}$$

 DOI 10.1007/s10040-005-0459-0

where H_1 is the subsidence due to the change in hydrous state (cm) and d_c is the original formation thickness (cm).

Subsidence due to interlayer dehydration

Ransom and Helgeson (1994a) described the thermodynamic characteristic of hydrated or dehydrated smectite as the possession or lack of interlayer water. The structure of 2:1-type smectite does not change during dehydration. The interlayer region in the silicate structure can be considered to be a solvent; the water is the solute dissolved in the solvent, and the solution is called a solid solution.

The chemical and thermodynamic properties of interlayer water differ from those of pore water. Interlayer water can be considered as water bonded to a mineral, forming a hydrated mineral. When dehydration occurs, the interlayer water will be released from the hydrated smectite to form H_2O and a homologous anhydrous 2:1 layer silicate counterpart. This behavior is analogous to the reversible intracrystallization reaction of a solid solution and is specified by the following equation (Ransom and Helgeson 1994a, 1995).

$$hs \overset{K}{\rightleftharpoons} as + n\mathrm{H_2O} \tag{12}$$

where *hs* denotes hydrous smectite; *as* denotes anhydrous smectite; n is the number of moles of water released from 1 mole of hydrous smectite, and K = thermodynamic equilibrium constant. Therefore, the reaction tends to move to the left when water content exceeds equilibrium (for example, before the end of primary consolidation), thereby generating a hydrous form of smectite with a higher volume than otherwise. After most of the pore water is slowly drained out, the reaction tends to move to the right until equilibrium is reached.

If the distribution of hydrous and anhydrous smectite is described as a mole fraction at equilibrium, then the thermodynamic equilibrium constant (K) in Eq. (12) can be expressed as,

$$K = \frac{a_{\mathrm{as}}\left(a_{\mathrm{H_2O}}\right)^n}{a_{\mathrm{hs}}} = \frac{X_{\mathrm{as}}\lambda_{\mathrm{as}}\left(a_{\mathrm{H_2O}}\right)^n}{X_{\mathrm{hs}}\lambda_{\mathrm{hs}}} \tag{13}$$

where a_i, x_i, λ_i represent the activity, mole fraction, and activity coefficient of component i, respectively. Assuming a binary system wherein only hydrous and anhydrous smectite components are present in solid solution, the sum of the mole fractions of hydrous and anhydrous smectite components equals one.

$$X_{\mathrm{hs}} + X_{\mathrm{as}} = 1 \tag{14}$$

Then, Eq. (12) can be rewritten as,

$$\log K = \log\left(\frac{1 - X_{\mathrm{hs}}}{X_{\mathrm{hs}}}\right) + \log\left(\frac{\lambda_{\mathrm{as}}}{\lambda_{\mathrm{hs}}}\right) + n \log a_{H_2O} \tag{15}$$

where, the ratio $\frac{\lambda_{\mathrm{as}}}{\lambda_{\mathrm{hs}}}$ was set to be constant by assuming that the effect of pressure on $\frac{\lambda_{\mathrm{as}}}{\lambda_{\mathrm{hs}}}$ is negligible.

A new parameter Φ is defined as following,

$$\Phi \equiv \log\left(\frac{1 - X_{\mathrm{hs}}}{X_{\mathrm{hs}}}\right) + n \log a_{\mathrm{H_2O}} \tag{16}$$

Applying regular solution theory (Anderson and Crerar 1993) to the hydrous and anhydrous smectite/water binary system, the Φ can be expressed as,

$$\Phi = \frac{-W_s}{2.30RT}(2X_{\mathrm{hs}} - 1) + \log K \tag{17}$$

where, W_s: Margule's parameter associated with the solid solution.

The value of Φ in Eq. (16) can be determined from X_{hs}. If the number of moles of water released per mole of hydrous smectite, n, is also known, a linear relationship between Φ (y axis) and ($2X_{\mathrm{hs}}-1$) (x axis) can be plotted, yielding a slope of $\frac{-W_s}{2.30\mathrm{RT}}$ and an intercept of $log\ K$.

Using $O_{10}(OH)_2$ as a base crystal chemical unit, Ransom and Helgeson (1989) expressed hydrated Na-smectite ($Na_{0.3}Al_{1.9}Si_4O_{10}(OH)_2nH_2O$, where n is the number of moles of water in the fully hydrated Na-smectite). In this paper this model also is adopted with the modification that Na-smectite is a solid solution with basal spacings from 10 Å to 19 Å. Na^+-rich seawater intrudes upon the coastal groundwater. Also, the assumption of Ransom and Helgeson (1989) is followed, that 2:1-type dioctahedral and trioctahedral Na-smectite exhibit the same thermodynamic solid solution properties.

The interlayer molar volume (V_{il}) can be determined by (Ransom and Helgeson 1994a)

$$V_{\mathrm{il}} = \left(\frac{abc \cdot \cos(90 - \beta)}{10^{24}Z}\right) N_0 \tag{18}$$

where, a=5.172 Å, b=8.985 Å and β=100Å are parameters associated with the smectite lattice unit; c is the interlayer thickness; Z=2 is the number of units in the chemical formula of the smectite lattice unit, and N_o is Avogadro's number. Based on the assumption of the structure of hydrous smectite, 1 mole O_{10} $(OH)_2$ and 0.3 mole Na^+ are always present in 1 mole hydrous smectite. The parameter c is set to 9 Å (19 Å−10 Å). Subtracting the molar volume of Na^+ (2.66 cm^3) from a hydrous smectite yields an interlayer water molar volume of 122.8 cm^3/mole. The number of moles of water released by the dehydration of hydrous smectite is thus,

$$n = \frac{\rho_{\mathrm{il}} V_{\mathrm{il}}}{M_w} \tag{19}$$

where ρ_{il} is the density of the interlayer water; M_w is the molecular weight of water and equals 18.05. Hawkins and Egelstaff (1980) measured the average interlayer water

 DOI 10.1007/s10040-005-0459-0

density as 1.05 g/cm. Substituting in values of ρ_{il} and M_w, gives n of 7.16. Defined in Eq. (17) , the slope of $\frac{-W_s}{2.30RT}$ is 2.02, the intercept of log K is –1.76 and X_{hs} equals 0.79.

Pressure dependent equilibrium constant

The thermodynamic solid solution model of the smectite dehydration reaction is derived at 25°C and 1 bar. The basal spacing ranges from 10 Å for complete dehydration to 19 Å at complete hydration. However, the pressure in the subsurface shallow sediment exceeds 1 bar; thus, the change in the equilibrium constant at various pressures must be derived.

According to chemical equilibrium, log K can be calculated from the change in Gibb's free energy ($G_{H_2O,P}$) at any temperature and pressure, by the following equation.

$$\log K = -\frac{1}{2.30RT}\Delta G_r^0 \tag{20}$$

where R and T denote the gas constant (8.31 J/mole k) and temperature (k), respectively. ΔG_r^0 is the reaction Gibb's free energy and may change with the environmental conditions (kcal/mole). The relationship between pressure change and ΔG_r^0 at the reference temperature (298.15 k) is,

$$\Delta G^o_{r,p} = \Delta G^o_{r,p_r} + \int_{p_r}^{p} \Delta V \, dP \tag{21}$$

where p_r is the reference pressure of 1 bar, (1 bar = 100 kPa), and P stands for any pressure of interest (kPa). ΔV is the volume change due to the release (or swelling) of water from 1 mole of soil particles when the pressure changes from p_r to p, and can be expressed as,

$$\begin{aligned}\Delta V &= (V^o_{hs,p} - V^o_{hs,p_r}) + (V^o_{as,p} - V^o_{as,p_r}) \\ &+7.16(V^o_{H_2O,p} - V^o_{H_2O,p_r})\end{aligned} \tag{22}$$

where $(V^o_{hs,p} - V^o_{hs,p_r})$ denotes the change in the molar volume of hydrous smectite as the pressure changes from p_r to p (cm^3/mole); $(V^o_{as,p} - V^o_{as,p_r})$ denotes the change in the molar volume of anhydrous smectite as the pressure changes from p_r to p (cm^3/mole), and $(V^o_{H_2O,p} - V^o_{H_2O,p_r})$ denotes the change in molar volume of water when the pressure changes from p_r to p (cm^3/mole).

Combining Eq. (18) with the calculated molar volume of hydrous smectite enables the $\int_{p_r}^{p} \Delta V \, dP$ part in Eq. (21) to be expressed as,

$$\begin{aligned}\int_{p_r}^{p} \Delta V \, dP &= \int_{p_r}^{p} \{13.73[c(P) - c(p_r)] \\ &+ 7.16(V^o_{H_2O,p} - V^o_{H_2O,p})\} dP \\ &= 13.73 \int_{p_r}^{p} [c(P) - c(p_r)] dP \\ &+ 7.16(G^o_{H_2O,p} - G^o_{H_2O,p}) \\ &- 7.16 \times V^o_{H_2O,p_r}(p - p_r)\end{aligned} \tag{23}$$

where $c(p_r)$ is the basal spacing at the reference pressure (p_r); $G^o_{H_2O,p}$ and $G^o_{H_2O,p_r}$ denote the standard molar Gibbs free energy of bulk water at pressures p and p_r, respectively. The values of ($G^o_{H_2O,p} - G^o_{H_2O,p_r}$) and $V^o_{H_2O,p_r}$ in this study were generated using the computer program SUPCRT92 (Johnson et al. 1992). Thus, Eqs. (21) and (23) can be used to compute the standard molar Gibbs free energy at a specific formation pressure; then Eq. (20) can be employed to determine the corresponding equilibrium constant K. Finally, Eq. (15) can be adopted to determine the mole fractions of hydrous and anhydrous smectite, $X_{hs,p}$, and $X_{as,p}$, respectively, at a formation pressure, p.

Equations (22) and (23) can be used to evaluate the standard Gibb's free energy of an increase in effective stress (P_P) caused by the over-pumping of groundwater. The corresponding equilibrium constant K can be computed using Eq. (21). Equation (15) then determines the hydrous and anhydrous mole fractions of smectite at P_P (X_{hs,P_P} and X_{as,P_P}, respectively). The mole fraction change due to smectite dehydration from P to P_P is,

$$\Delta X_{as} = X_{as,P} - X_{as,P_P} \tag{24}$$

Thus, the land subsidence caused by over-pumping required to trigger the dehydration of smectite is,

$$H_2 = \frac{\Delta X_{as} \times V_{cw} \times d_c \times P_s}{V_c} \tag{25}$$

where, H_2: amount of land subsidence estimated using the theory of the interlayer dehydration of solid solution (cm), V_{cw}: water volume per mole of smectite (122.8 cm^3/mol), d_c: original thickness of formation (cm), P_s: proportion of smectite in a clay system, ΔX_{as}: mole fraction of anhydrous smectite due to dehydration of smectite, V_c: molar volume of anhydrous smectite (260.67 cm^3/mol).

This study, adopts Montana II($Na_{0.76}(Al_{1.51}Mg_{0.19}Fe^{3+}{}_{0.23})(Al_{0.34}Si_{3.66})O_{10}(OH)_2 4.5H_2O$ as defined by Eslinger et al. (1979), of which the molar volume is 215.36 cm^3/mol (Ransom and Helgeson 1994b); changes the amount of interlayer water from 4.5 to 7.16 mole and modifies V_c 260.67 cm^3/mol).

The overall subsidence (H) caused by the dehydration following the over-pumping of groundwater is the summation of the subsidence due to the change in interlayer hydration state (H_1) and the subsidence due to interlayer dehydration (H_2)

$$H = H_1 + H_2 \tag{26}$$

These two models are applied to evaluate the effect of smectite dehydration on the cumulative amount of land subsidence in the Chang Hua and Yun Lin coastal areas of the Chou-Shui River alluvial fan and the Yun Lin offshore industrial infrastructure complex.

 DOI 10.1007/s10040-005-0459-0

Subsidence in the coastal area of Chou-Shiu River alluvial fan

Description of study area

The Chou-Shui River alluvial fan is located on the western coast of Taiwan, and covers the plain of Chang Hua, Yun Lin, and the northern part of the Chia Yi counties, as depicted in Fig. 1. The alluvial fan is enclosed by the Taiwan Strait to the west, by the Wu River to the north, by the Dulliu Hill and Baguah Mount to the east, and by the Peikang River to the south. The alluvial fan has an area of approximately 1,800 km^2 and is broadly partitioned into the proximal-fan, mid-fan and distal-fan areas. Unconsolidated sediments that underlie the alluvial fan contain much groundwater and are of late Quaternary age. The proximal-fan is a major recharge region for the aquifers. The long-term average amounts of groundwater pumped and recharged from 1970 to 1990 were 1.326 and 1.024 billion m^3/yr, respectively. These statistics indicate that a substantial amount of groundwater was over drafted from the aquifers (Central Geological Survey 1999). Groundwater levels fell markedly from 1970 to 1990 but recovered slightly after 1991.

Drilling and stratigraphic analyses of the subsurface geology were conducted between 1992 and 1998 to understand further the hydro geological characteristics of the alluvial fan. A new groundwater monitoring network, including 77 hydro geological investigation stations and 188 groundwater monitoring wells in different aquifers (Taiwan Sugar Corporation 1997), was quickly established. Subsurface hydro geological analysis to a depth of around 300 m can be divided into 6 overlapping sequences, including three marine sequences and three non-marine sequences, in the distal-fan and mid-fan areas (Central Geological Survey 1999). Generally, non-marine sequences of formations, with coarse sediment sizes ranging from that of medium sand to that of gravel with high permeability, can be considered as aquifers, whereas the marine sequences of formations, with fine sediment sizes ranging from that of clay to that of fine sand of low permeability can be considered as aquitards (Fig. 4).

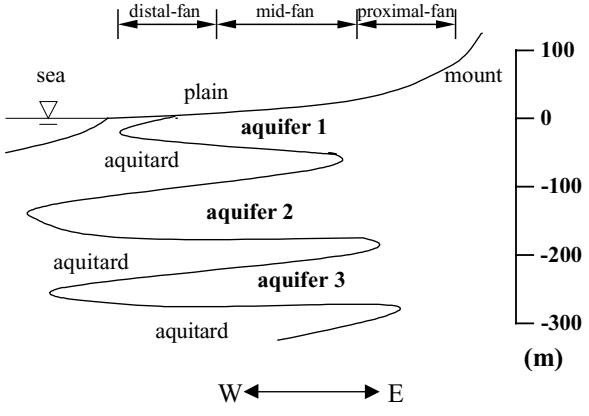

Fig. 4 Conceptual hydrogeological profile of Chou-Shui River alluvial fan

The hydro geological proximal-fan formation, which is primarily composed of gravel and sand, is regarded as an unconfined aquifer. The aquitards in the distal-fan and mid-fan areas gradually diminish in thickness toward the east. The conceptual hydrogeological profile suggests that highly permeable materials are assumed to be present in the extended aquitards of the proximal-fan area. The upper aquifer is then labeled "aquifer 1". The intermediate aquifer is labeled "aquifer 2". Finally, the lower aquifer is labeled "aquifer 3" (Water Resources Bureau 2001b)

Subsidence monitoring data

The Water Resources Bureau of the Ministry of Economic Affairs has conducted a long term land subsidence survey in the coastal area of the Chou-Shui River alluvial fan (Water Resources Bureau 2001a). The major area of subsidence was centered on Lu-Kong before 1990 and gradually moved to the south region of Chang Hua (Water Resources Bureau 1997). In 1997, Shi-Kong was area of the most serious subsidence. The average annual subsidence was 16–24 cm in 1995–1997 and decreased to 8–11 cm/yr in 1998–2000. The annual rate of land subsidence exceeds 5 cm south of Lu-Kong and exceeds 10 cm around Shi-Kong. The area of subsidence has become larger since 1991, and by 1998 the rate of subsidence exceeded 10 cm/yr over an area of about 100.5 km^2.

Subsidence at Yun Lin began in 1970. Before 1980, the region of subsidence was limited within the King-Hu area. In 1980, the region of land subsidence extended to the Tai-Shi area and in 1987 the land subsidence further expanded to the estuary of the Chou-Shiu River. The cumulative land subsidence from 1976 to 2000 at Mai-Liao, King-Hu, Tai-Shi and Yi-Wu were 92, 195, 208 and 188 cm, respectively. By 1998, the annual land subsidence exceeded 10 cm/yr in the Yun Lin coastal area of approximately 120 km^2. Based on multi-level data from subsidence-monitoring wells, most land subsidence occurred in the strata between 55 m and 94 m (Water Resources Bureau 2001a). This finding is consistent with the hypothesis that the over-pumping of groundwater is the main contributor to land subsidence, since groundwater is primarily withdrawn from aquifers at a depth of 50 m below the ground surface in that region.

Subsidence due to smectite dehydration

Based on the developed model of the hydration state of smectite and the solid solution model of smectite dehydration, subsidence due to smectite dehydration in Shi-Kong, Mai-Liao, Tai-Shi and Yi-Wu is quantified.

Shi-Kong

Figure 5 illustrates the stratigraphic core sequence observed in the land subsidence-monitoring well in Shi-Kong. The strata are divided into 30 parts. Table 1 lists the physical properties of each part. The original level of the groundwater was 4.2 m above mean sea level in 1968 and decreased significantly due to the over-pumping of groundwater. By

DOI 10.1007/s10040-005-0459-0

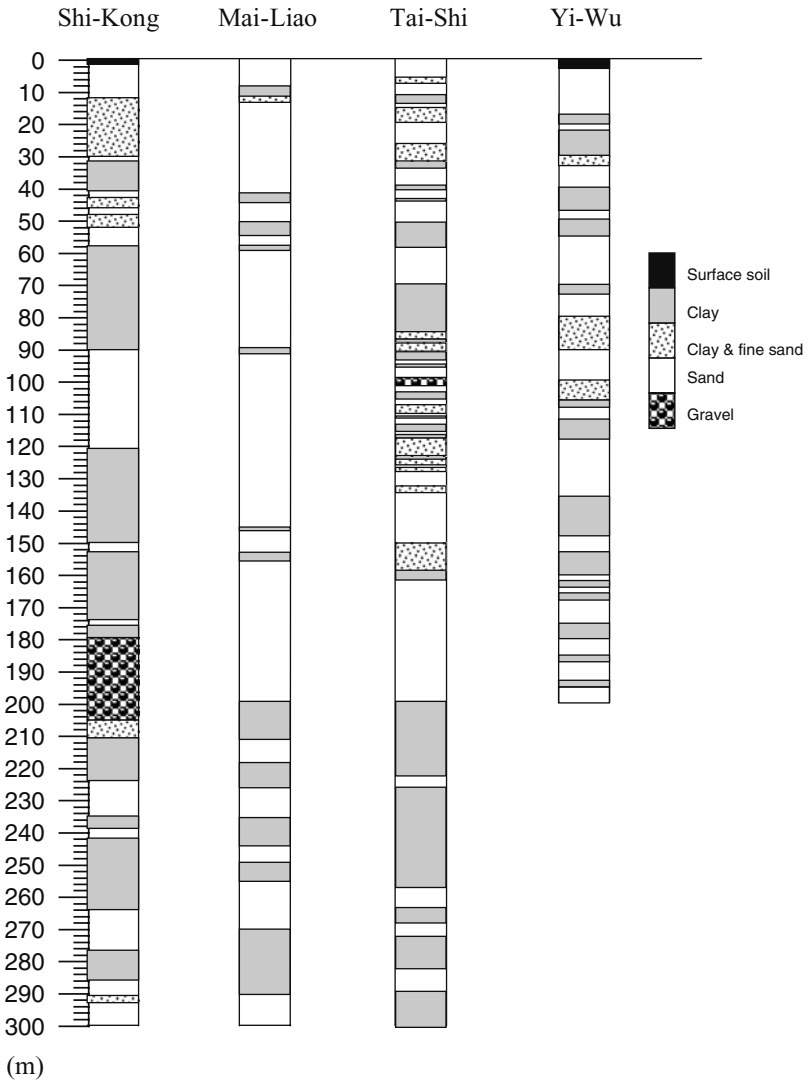

Fig. 5 Schematic illustration of the stratigraphic profiles of Shi-Kong, Mai-Liao, Tai-Shi and Yi-Wu (Water Resources Bureau 2001a)

2000, the multilevel monitoring well recorded groundwater levels of –16.68, –32.5, –15.93 and –4.92 m at depths of 55, 94, 206 and 268 m, respectively. The decline in groundwater level increased the effective stress on the strata, as presented in Table 2.

The 30 stratigraphic samples, labeled I-1 to I-30, from Shi-Kong were grouped into 16 sublayers by classifying the subsurface soil as clay, clay/fine sand or gravel. Table 3 shows the computed subsidence results of the corresponding sub layers due to smectite dehydration. In samples I-2 to I-7, a total of four sub layers meet Condition 1 in the model in this study, where the effective stress to which the strata are originally subjected was less than 740.95 kPa, and the increased effective stress due to pumping remains under 740.95 kPa. The hydration state following the dehydration of smectite is evaluated using the model of the hydration state of smectite. Samples I-8 to I-10 meet Condition 2 of the model in this study, where the effective stress to which they were originally subjected after pumping exceeds 740.95 kPa, which facilitates the passing of the smectite hydration state across the discontinuous jump in the basal spacing. The effects of smectite dehydration must be evaluated using both the model of the hydration state of smectite and the solid solution model of smectite dehydration. Samples I-12 to I-29 include 10 sublayers which meet Condition 3 of the model in this study, where the original subjected effective stress of the strata exceeds 740.95 kPa; that is the original effective stress in the strata before pumping has already crossed the discontinuous jump in the basal spacing and it leads to chemical equilibrium. Thus, the subsidence is quantified using the solid solution model of smectite dehydration. The estimated subsidence of the 16 sublayers, due to smectite dehydration, is 23.23 cm (see Table 3).

Mai-Liao, Tai-Shi and Yi-Wu

The subsidence in the other three study areas, Mai-Liao, Tai-Shi and Yi-Wu were computed by the same procedure as that used by Shi-Kong. The original groundwater level before land subsidence was 3.78 m above mean sea level in Mai-Liao in 1968. By 2000, the multilevel monitoring well recorded groundwater levels at depths of 110 and 179 m that

 DOI 10.1007/s10040-005-0459-0

Table 1 Physical properties of the soil formation in Shi-Kong

Depth (m)	Sieve analysis (%)				Specific weight	Void ratio	Weight (%)	LL[a](%)	C_c[b]
	Gravel	Sand	Silt	Clay					
2.5–3.4	0	88	12	0	2.67	0.61	17.96	–	0.13
9.0–9.9	0	97	3	0	2.65	0.79	26.26	–	0.25
21.1–21.9	0	8	61	31	2.72	0.96	35.42	39	0.28
30.0–30.9	0	82	18	0	2.65	0.81	30.64	–	0.19
48.0–48.9	0	70	30	0	2.67	0.76	28.60	–	0.21
34–35	0	8	76	16	2.68	–	6.63	29.3	–
35–36	0	0	70	30	2.72	–	23.36	27.8	–
53–54	0	96	4	0	2.73	–	20.38	–	–
54–55	0	96	4	0	2.71	–	19.24	–	–
79–80	0	0	66	34	2.69	–	20.57	38.2	–
80–81	0	6	70	24	2.66	–	19.47	29.5	–
97–98	1	98	1	0	2.68	–	20.1	–	–
98–99	2	85	13	0	2.70	–	20.04	–	–
139–140	0	0	48	52	2.70	–	30.17	40.9	–
140–141	0	0	78	22	2.71	–	26.05	25.8	–
159–160	0	7	66	27	2.72	–	18.46	26.4	–
160–161	0	22	54	24	2.71	–	18.60	20.4	–
189–190	1	95	4	0	2.71	–	22.71	–	–
190–191	1	95	4	0	2.71	–	12.52	–	–
267–268	0	95	5	0	2.73	–	18.78	–	–
268–269	0	96	4	0	2.70	–	17.92	–	–
279–280	0	0	67	33	2.71	–	28.08	33.9	–
280–281	0	0	67	33	2.73	–	29.51	34.7	–
296–297	0	95	5	0	2.69	–	26.25	–	–
297–298	0	93	7	0	2.75	–	24.87	–	–

[a]LL: Liquid limit

[b]C_c: Coefficient of compressibility

had dropped to –18.35 m and –18.65 m, respectively. The 26 stratigraphic samples, labeled II-1 to II-26, in Mai-Liao were grouped into 13 sublayers by classifying them as clay, clay/fine sand or sand. Samples II-2 to II-5 with a total of three sublayers meet Condition 1 in the model in this study, Samples II-7 to II-9 meet Condition 2, Samples II-11 to II-25 with a total of eight sublayers, meet the Condition 3. The total estimated subsidence of the 13 sublayers due to smectite dehydration is 20.98 cm.

The original groundwater level before land subsidence was 0 m in Tai-Shi in 1968. By 2000, the observed groundwater levels in the multilevel monitoring well were −8, −17.2, −17.2 and –10 m, respectively, at depths of 49, 105, 203 and 282 m. The 58 stratigraphic samples, numbered III-1 to III-58 in Tai-Shi are grouped into 33 sublayers by classification as clay, clay/fine sand, sand and gravel. Samples III-2 to III-15 with a total of eight sublayers, meet the Condition 1, III-16 meet the Condition 2, III-18 to III-58 with a total of 24 sublayers, meet Condition 3. The total estimated subsidence of the 33 sublayers due to smectite dehydration is 19.88 cm.

The original groundwater level before land subsidence was –6.44 m in Yi-Wu in 1968. By 2000, the observed groundwater levels in the multilevel monitoring well were –23.37, -27.52, -25.04 and –23.76 m at depths of 96, 161, 171 and 219 m, respectively. The 33 stratigraphic samples, numbered IV-1 to IV-33, are grouped into 17 sublayers by classifying the soil or clay, clay/fine sand or sand. Samples IV-2 to IV-9 with a total of five sublayers meet Condition 1, samples IV-11 to IV-32 with a total of 12 sublayers meet Condition 3. The total estimated subsidence of the 17 sublayers caused by smectite dehydration is 17.77 cm.

Comparison

The subsidence determined from smectite dehydration caused by the over-pumping of groundwater in Shi-Kong (depth of 300 m), Mai-Liao (depth of 300 m), Tai-Shi (depth of 300 m) and Yi-Wu (depth of 200 m) are 23.23, 20.98, 19.88 and 17.79 cm, respectively. The amount of subsidence resulting from the solid solution model of smectite dehydration, when the effective stress applied to the strata exceeds 740.95 kPa after over-pumping in Shi-Kong, Mai-Liao, Tai-Shi and Yi-Wu, are 0.454 cm, 1.066 cm, 0.108 cm and 0.002 cm, respectively, representing only 1.95, 5.08, 0.54 and 0.01% of overall subsidence caused by smectite dehydration.

Figures 6–9 show plots of measured cumulated subsidence and computed land subsidence from smectite dehydration, against depth in Shi-Kong, Mai-Liao, Tai-Shi and Yi-Wu. The results indicate that the major land subsidence caused by smectite dehydration occurs in shallow subsurface formations (−0 to 60 m depth) whereas only a small amount of land subsidence caused by smectite dehydration was present at a depth of over 60 m. The increase in the effective stress by the fall in groundwater level is not sufficient to enable the release of water in the smectite interlayer in a deeper subsurface formation.

 DOI 10.1007/s10040-005-0459-0

Table 2 Initial effective stress applied to sublayer soil and the increase in effective stress caused by the drawdown of groundwater level

Number	Depth (m)	Thickness (m)	Formation type	Effective stress applied to strata (kPa) (1)	Effective stress increased by drawdown of groundwater (kPa) (2)	Cumulative effective stress (kPa) (1)+(2)
I-1	0.00–11.00	11	Sand	72.55	–	–
I-2	11.00—30.00	19	Clay/fine sand	260.90	204.83	465.73
I-3	30.00–32.00	2	Sand	389.89	–	–
I-4	32.00–34.00	2	Clay	413.27	204.83	618.10
I-5	34.00–41.00	7	Clay	459.13	204.83	663.96
I-6	41.00–43.00	2	Sand	507.98	–	–
I-7	43.00–46.00	2.2	Clay/fine sand	534.58	204.83	739.41
I-8	43.00–46.00	0.8	Clay/fine sand	552.86	204.83	757.70
I-9	46.00–49.00	3	Sand	567.77	–	–
I-10	49.00–52.00	3	Clay/fine sand	615.60	204.83	820.43
I-11	52.00–58.00	6	Sand	663.70	–	–
I-12	58.00–90.00	32	Clay	876.06	360.03	1236.09
I-13	90.00–121.00	31	Sand	1233.79	–	–
I-14	121.00–150.00	29	Clay	1595.75	360.03	1955.77
I-15	150.00–153.00	3	Sand	1753.53	–	–
I-16	153.00–174.00	21	Clay	1890.07	197.48	2087.54
I-17	174.00–176.00	2	Sand	2000.50	–	–
I-18	176.00–180.00	4	Clay	2043.82	197.48	2241.30
I-19	180.00–205.00	25	Sand	2219.32	–	–
I-20	205.00–211.00	6	Clay/fine sand	2430.52	89.47	2519.99
I-21	211.00–224.00	13	Clay	2533.33	89.47	2622.79
I-22	224.00–235.00	11	Sand	2662.35	–	–
I-23	235.00–239.00	4	Clay	2765.03	89.47	2854.50
I-24	239.00–242.00	3	Sand	2795.44	–	–
I-25	242.00–264.00	22	Clay	2937.07	89.47	3026.54
I-26	264.00–277.00	13	Sand	3125.14	–	–
I-27	277.00–286.00	9	Clay	3266.49	89.47	3355.95
I-28	286.00–291.00	5	Sand	3335.56	–	–
I-29	291.00–293.00	2	Clay/fine sand	3390.48	89.47	3479.95
I-30	293.00–300.00	7	Sand	3439.08	–	–

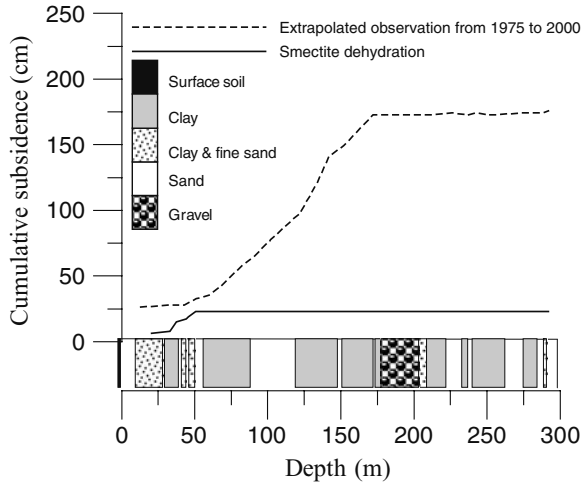

Fig. 6 Cumulative land subsidence versus depth at Shi-Kong

Recall that Fig. 3 presents the relationships among m_w/m_c, the basal spacing and the swelling pressure of Na-smectite at 25°C. As m_w/m_c decreases from 5 to 1.5 g/g, the swelling pressure of smectite increases from 64.94 kPa to 740.95 kPa, and the basal spacing decreases from ∼110 Å to ∼43 Å. If the applied effective stress further increases, the swelling pressure drops fast, even to a negative pressure, triggering a discontinuous jump in the basal spacing at m_w/m_c (∼1.0 g/g). The basal spacing will fall continuously from −43 Å to 19 Å. Thus, the applied effective stress on the strata increases from 64.94 kPa to 740.95 kPa, and the interlayer basal spacing of hydrated smectite can decrease from ∼110 Å to ∼19 Å, yielding a 91 Å spacing difference. If the original effective stress applied to strata exceeds 740.95 kPa and the solid solution model of smectite dehydration is adopted to evaluate the subsidence caused by smectite dehydration (Fig. 3), then as the swelling pressure increases from 740.95 kPa to 6500 kPa (∼300 m depth) the basal spacing only decreases from ∼19 Å to 16.9 Å, giving a 2.1 Å spacing difference. Restated, the basal spacing change by only 2.26% as the effective stress increases from 740.95 kPa to 6500 kPa, but it changes by 97.74% as the effective stress increases from 64.94 kPa to 740.95 kPa. The 2.26% change was

 DOI 10.1007/s10040-005-0459-0

Table 3 Computed land subsidence from the release of smectite interlayer water in Shi-Kong

Field derived data							Calculated results						
Stratum number	Depth range (m)	Thickness (m)	Smectite clay (%)	W_c (g/g)	P (kPa)	ρ_b (g/cm^3)	$\bar{m}(P)$ (g/g)	α_p (g/g)	P_p (kPa)	$\bar{m}(P_p)$ (g/g)	α_{p_p} (g/g)	$\Delta\phi$	H_1 (cm)
I-2	11.00–30.00	19	0.27	0.17	260.90	2.24	2.49	0.71	465.73	1.82	0.65	0.003	6.56
I-4	32.00–34.00	2	1.27	0.23	413.27	2.04	1.94	0.66	618.10	1.60	0.62	0.007	1.42
I-5	34.00–41.00	7	2.18	0.22	459.13	2.04	1.84	0.65	663.96	1.56	0.61	0.010	7.18
I-7	43.00–45.20	2.2	2.74	0.22	534.58	2.24	1.71	0.63	739.41	1.49	0.60	0.011	2.36
I-8	45.20–46.00	0.8	1.10	0.22	552.86	2.24	1.68	0.63	757.70	1.00	0.50	0.014	1.11
I-10	49.00–52.00	3	1.23	0.20	615.60	2.24	1.60	0.62	820.43	1.00	0.50	0.014	4.15
												ΣH_1 =22.78	
Stratum number	Depth range (m)	Thickness (m)	Smectite clay (%)	P (kPa)	$\Delta G^o_{r,p}$ (kcal/mole)	$X_{as,p}$	P_p (kPa)	$\Delta G^o_{r,p_p}$ (kcal/mole)	X_{as,p_p}	ΔX_{as}	H_2 (cm)		
I-8	45.20–46.00	0.8	1.10	552.86	–	–	757.70	2.40	0.21	0.21	0.09		
I-10	49.00–52.00	3	1.23	615.60	–	–	820.43	2.40	0.21	0.21	0.36		
I-12	58.00–90.00	32	1.81	876.06	2.40	0.21	1236.09	2.40	0.21	0.00	0.00		
I-14	121.00–150.00	29	1.76	1595.75	2.40	0.21	1955.77	2.40	0.21	0.00	0.00		
I-16	153.00–174.00	21	1.47	1890.07	2.40	0.21	2087.54	2.40	0.21	0.00	0.00		
I-18	176.00–180.00	4	1.48	2043.82	2.40	0.21	2241.30	2.40	0.21	0.00	0.00		
I-20	205.00–211.00	6	1.39	2430.52	2.40	0.21	2519.99	2.40	0.21	0.00	0.00		
I-21	211.00–224.00	13	1.51	2533.33	2.40	0.21	2622.79	2.40	0.21	0.00	0.00		
I-23	235.00–239.00	4	1.26	2765.03	2.40	0.21	2854.50	2.40	0.21	0.00	0.00		
I-25	242.00–264.00	22	0.80	2937.07	2.40	0.21	3026.54	2.40	0.21	0.00	0.00		
I-27	277.00–286.00	9	2.61	3266.49	2.40	0.21	3355.95	2.39	0.21	0.00	0.00		
I-29	291.00–293.00	2	1.24	3390.48	2.39	0.21	3479.95	2.39	0.21	0.00	0.00		
									ΣH_2 = 0.45	$\Sigma H_1+H_2=H$ = 23.23			

DOI 10.1007/s10040-005-0459-0

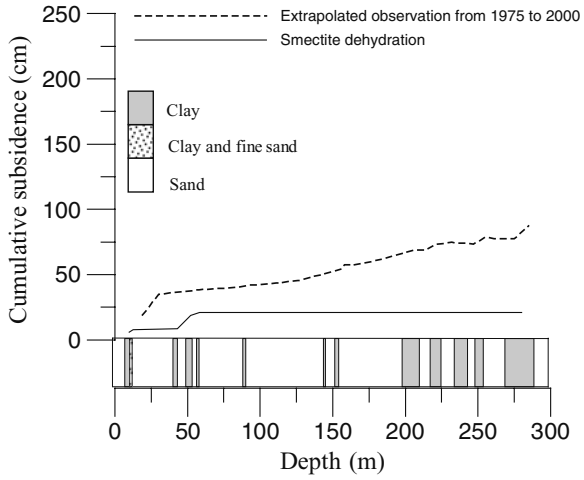

Fig. 7 Cumulative land subsidence versus depth at Mai-Liao

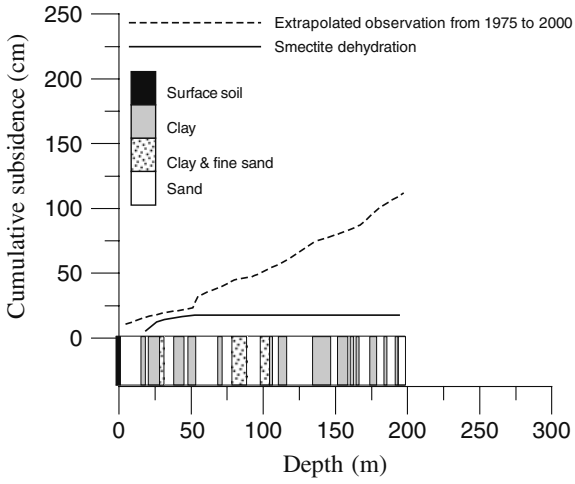

Fig. 9 Cumulative land subsidence versus depth at Yi-Wu

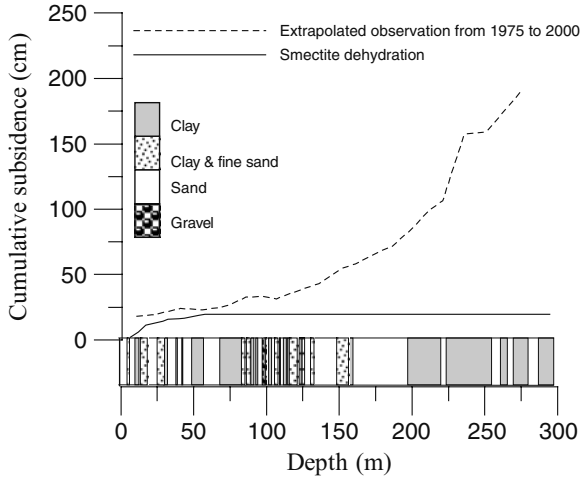

Fig. 8 Cumulative land subsidence versus depth at Tai-Shi

close to the 1.9% value obtained by taking the average of the values at the above four subsidence locations.

The data obtained at the multilevel land subsidence monitoring wells from 1975 to 2000, and the benchmark measurements of the ground surface in 1975, 1989 and 2000 indicate that the accumulated land subsidence (in Shi-Kong, Mai-Liao, Tai-Shi and Yi-Wu) from 1975 to 2000 is 185, 92, 208 and 188 cm. The estimated land subsidence by smectite dehydration resulting from over-pumping in Shi-Kong, Mai-Liao, Tai-Shi and Yi-Wu is 12.56, 22.80, 9.56 and 9.45%, respectively, of the accumulated land subsidence measured in the field.

Subsidence in Yun Lin offshore industrial infrastructure complex

The Yun Lin offshore industrial infrastructure complex is developed by pumping ocean sand to construct offshore land for industrial needs (Fig. 1). The Industry Bureau estimated that the surface subsidence of the new land was 60–70 cm in the first year, less than 10 cm in the fourth year and will become stabilized to a negligible value after the fifth year. The analysis by the Industry Bureau did not account for the effect of smectite dehydration on the subsidence of the land (Industry Bureau 2000). Given the stratigraphic core sequence and the soil's mechanical properties recorded at the land subsidence monitoring well in the Shi-Shi district, Terzaghi's (1943) one-dimensional compaction theory is employed to compute the land subsidence caused by primary consolidation in a layered formation and that caused by smectite dehydration.

Table 4 presents computed results obtained using Terzaghi's one dimensional compaction theory; the total final cumulative subsidence of a 200 m thick offshore formation is 69.64 cm. The amount of subsidence is 66.16 cm over a compacting time of 285.5 days, comprising 95% of the final accumulative subsidence. The subsidence becomes 69.40 cm after 900 days (or 2.5 years) of compaction, and then reaches its final value of subsidence. Figure 10 is a plot of the measured land subsidence and the computed land subsidence, against time, according to Terzaghi's compaction theory, for a 200 m deep formation. The measured land subsidence does not stabilize after the fifth year whereas the computed land subsidence stabilizes after around 2.5 years. The difference between the measured and computed stable land subsidence is 32.75 cm. Notably, using the smectite dehydration model, the computed land subsidence caused by smectite dehydration is 30.07 cm, as shown in Table 5, which is close to the underestimate of 32.75 cm, obtained using Terzaghi compaction theory. Including the effect of smectite dehydration on subsidence yields a computed result that agrees well with the measured subsidence data.

Discussion

Residual water in interlayer of smectite

As the smectite dehydration reaction caused by pumping reaches chemical equilibrium, changing other

 DOI 10.1007/s10040-005-0459-0

Table 4 Land subsidence computed by applying Terzaghi's compaction theory to the Yun Lin offshore industrial infrastructure complex (Industry Bureau 2000)

Number	Soil type	Depth range (m)	Thickness (m)	Soil specific weight (t/m^3)	Void ratio e	C_c	Original effective stress (t/m^2)	Increment effective stress (t/m^2)	Final compacted subsidence (cm)	Compaction coefficient (cm^2/s)	Subsidence in 285.5 days (cm)
1	Clay/fine sand	9.30–14.13	4.83	0.91	0.77	0.27	10.38	7.51	**17.41**	0.005	**17.28**
2	Clay/fine sand	15.20–18.20	3.00	1.03	0.66	0.27	15.14	7.51	**8.53**	0.005	**14.99**
3	Fine sand	18.20–21.28	3.08	0.94	0.76	0.27	18.13	7.50	**7.11**	0.005	
4	Fine sand	24.53–26.03	1.50	1.05	0.69	0.27	23.42	7.50	**2.89**	0.005	**2.89**
5	Clay	32.78–38.20	5.42	0.90	0.90	0.40	31.17	7.50	**10.68**	0.005	**10.48**
6	Fine sand	43.28–45.00	1.72	0.68	0.68	0.27	36.53	7.49	**2.24**	0.005	**2.72**
7	Fine sand	45.00–45.53	0.53	0.85	1.02	0.23	37.34	7.49	**0.48**	0.005	
8	Fine sand	47.03–49.00	1.97	0.80	1.00	0.23	39.50	7.48	**1.71**	0.005	**1.71**
9	Clay/fine sand	52.40–59.20	6.80	0.98	0.71	0.23	46.74	7.47	**5.89**	0.005	**5.45**
10	Fine sand	69.50–73.28	3.78	0.97	0.71	0.14	63.03	7.44	**1.50**	0.005	**3.27**
11	Fine sand	73.28–79.28	6.00	0.93	0.83	0.20	67.66	7.42	**2.96**	0.005	
12	Fine sand	79.28–81.00	1.72	0.92	0.78	0.14	71.24	7.41	**0.58**	0.005	
13	Fine sand	88.70–92.28	3.58	0.98	0.72	0.20	82.10	7.37	**1.55**	0.005	**1.55**
14	Fine sand	106.10–111.10	5.00	0.98	0.64	0.14	101.51	7.28	**1.28**	0.005	**1.27**
15	Clay	137.30–144.20	6.90	0.99	0.73	0.19	139.34	7.06	**1.63**	0.005	**1.50**
16	Clay	149.10–150.00	0.9	0.99	0.73	0.19	149.17	6.98	**0.20**	0.005	**0.20**
17	-	150.00–200.00	–	—	–	–	–	5.20	**3.00**	0.005	**2.85**
Total:									69.64 cm		66.16 cm

Total: 69.64 cm; Total: 66.16 cm

DOI 10.1007/s10040-005-0459-0

Table 5 Land subsidence computed from the release of water in the smectite interlayer caused by the overburden pressure in the Yun Lin offshore industrial infrastructure complex

Field derived data							Calculated results						
Stratum number	Depth range (m)	Thickness (m)	Smectite clay (%)	W_c (g/g)	P (kPa)	ρ_b (g/cm^3)	$\bar{m}(P)$ (g/g)	α_p (g/g)	P_p (kPa)	$\bar{m}(P_p)$ (g/g)	α_{p_p} (g/g)	$\Delta\phi$	H_1(cm)
1	9.30–14.13	4.83	0.94	0.30	101.83	2.10	4.12	0.80	175.50	3.11	0.76	0.015	7.39
2	15.20–18.20	3.00	1.12	0.30	148.52	2.10	3.40	0.77	222.20	2.73	0.73	0.012	3.66
3	18.20–21.28	3.08	1.27	0.30	177.86	2.10	3.09	0.76	251.43	2.54	0.72	0.011	3.42
4	24.53–26.03	1.50	1.27	0.30	229.75	2.10	2.68	0.73	303.33	2.29	0.70	0.008	1.19
5	32.78–38.20	5.42	2.70	0.30	305.78	2.10	2.28	0.70	379.35	2.03	0.67	0.011	5.99
6	43.28–45.00	1.72	1.72	0.30	358.36	2.10	2.09	0.68	431.84	1.90	0.65	0.005	0.94
7	45.00–45.53	0.53	1.72	0.30	366.31	2.10	2.07	0.67	439.78	1.88	0.65	0.005	0.28
8	47.03–49.00	1.97	1.23	0.30	387.50	2.10	2.01	0.67	460.87	1.83	0.65	0.003	0.67
9	52.40–59.20	6.80	1.18	0.30	458.52	2.10	1.84	0.65	531.80	1.71	0.63	0.002	1.64
10	69.50–73.28	3.78	1.81	0.30	618.32	2.10	1.60	0.62	691.31	1.53	0.61	0.002	0.77
11	73.28–79.28	6.00	1.81	0.30	663.74	2.10	1.56	0.61	736.53	1.50	0.60	0.002	1.04
12	79.28–81.00	1.72	1.81	0.30	698.86	2.10	1.53	0.60	771.56	1.00	0.50	0.015	2.65
												$\Sigma H_1 = 29.65$	
Stratum number	Depth range (m)	Thickness (m)	Smectite clay (%)	P (kPa)	$\Delta G^o_{r,p}$ (kcal/mole)	$X_{as,p}$	P_p (kPa)	$\Delta G^o_{r,p_p}$ (kcal/mole)	X_{as,p_p}	ΔX_{as}	H_2 (cm)		
12	79.28–81.00	1.72	1.18	698.86	–	–	771.56	2.396	0.209	0.209	0.420		
13	88.70–92.28	3.58	1.81	805.40	2.396	0.209	877.70	2.396	0.209	0.000	0.000		
14	106.10–111.10	5.00	2.75	995.81	2.396	0.209	1067.23	2.396	0.209	0.000	0.000		
15	137.30–144.20	6.90	3.39	1366.93	2.396	0.209	1436.18	2.396	0.209	0.000	0.000		
16	149.10–150.00	0.90	2.14	1463.36	2.396	0.209	1531.83	2.396	0.209	0.000	0.000		
										$\Sigma H_2 = 0.42$	$\Sigma H_1+H_2=H=30.07$		

DOI 10.1007/s10040-005-0459-0

Table 6 Computed land subsidence caused by complete release of water from the smectite interlayer in Shi-Kong

Field derived data						Calculated results					
Stratum number	Depth range (m)	Thickness (m)	Smectite clay (%)	W_c (g/g)	P (kPa)	$\bar{m}$ (P)(g/g)α_1 (g/g)	$\bar{m}_2$ (g/g)	α_2 (g/g)	$\Delta\phi$	H_1 (cm)	
I-2	11.00–30.00	19	0.27	0.17	260.90	2.49	0.71	1.00	0.50	0.008	14.65
I-4	32.00–34.00	2	1.27	0.23	413.27	1.94	0.66	1.00	0.50	0.020	3.95
I-5	34.00–41.00	7	2.18	0.22	459.13	1.84	0.65	1.00	0.50	0.030	21.36
I-7	43.00–45.20	2.2	2.74	0.22	534.58	1.71	0.63	1.00	0.50	0.036	7.84
I-8	45.20–46.00	0.8	1.10	0.22	552.86	1.68	0.63	1.00	0.50	0.014	1.11
I-10	49.00–52.00	3	1.23	0.20	615.60	1.60	0.62	1.00	0.50	0.014	4.15
										$\Sigma H_1 =$ 53.06	
Stratum number	Depth range (m)	Thickness (m)	Smectite clay(%)	ΔX_{as}	H_2 (cm)						
I-2	11.00–30.00	19	0.27	1	2.42						
I-4	32.00–34.00	2	1.27	1	1.20						
I-5	34.00–41.00	7	2.18	1	7.19						
I-7	43.00–45.20	2.2	2.74	1	2.84						
I-8	45.20–46.00	0.8	1.10	1	0.42						
I-10	49.00–52.00	3	1.23	1	1.74						
I-12	58.00–90.00	32	1.81	1	27.32						
I-14	121.00–150.00	29	1.76	1	24.08						
I-18	176.00–180.00	4	1.48	1	2.80						
I-20	205.00–211.00	6	1.39	1	3.93						
I-21	211.00–224.00	13	1.51	1	9.27						
I-23	235.00–239.00	4	1.26	1	2.36						
I-25	242.00–264.00	22	0.80	1	8.26						
I-27	277.00–286.00	9	2.61	1	11.09						
I-29	0.00	2	1.24	1	1.17						
					$\Sigma H_2 =$ 120.62						
					$\Sigma H_1+H_2=H$ = 173.67						

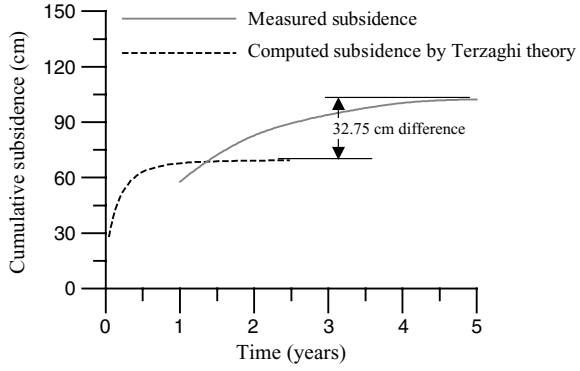

Fig. 10 Comparison of the measured land subsidence and land subsidence computed using Terzaghi theory at a depth of 0–200 m in the Yun Lin offshore industrial infrastructure complex

environmental parameters such as the increasing temperature or pressure, will break the chemical equilibrium, release water from the interlayer and produce further land subsidence. If the interlayer water of smectite is completely released, then the maximum subsidence caused by smectite dehydration in Shi-Kong (0–300 m), Mai-Liao (0–300 m), Tai-Shi (0–300 m) and Yi-Wu (0–200 m) is 173.67, 95.76, 242.42 and 147.11 cm, respectively. Table 6 details the calculated result of Shi-Kong as an example. The high subsidence in Tai-Shi is attributed to the high smectite content in the formation. After the water in the smectite interlayer is completely removed, the basal spacing is reduced to 10 Å. In the ambient pressure (1 bar) environment, the temperature must be increased to 300°C to complete dehydration (Bray et al. 1998). Such an increase in pressure is unlikely in the Chou-Shui River alluvial fan. Thus, the complete removal of interlayer water is not possible in the coastal region of the Chou-Shui River alluvial fan.

Transition of smectite to illite

Powers (1967), Bethke (1986), Audet and Fowler (1992) and Audet (1995) have examined the petrogenesis of smectite dehydration in which the basal spacing of smectite decreases from ~18.5 through ~15.5 and ~12 to ~10 Å and then the smectite transitions to illite. The transition breaks down the sedimentary structure and

 DOI 10.1007/s10040-005-0459-0

causes subsidence. Freed and Peacor (1989) and Pearson and Small (1988) found that the transition of smectite to illite occurs at a formation depth of 1.5 to 3.5 km and a temperature between 69 and 116°C. Elliott and Matisoff (1996) found that 20,000 years were required to transform completely smectite to illite at the depth of 2–4 km at a geothermal gradient of 76°C/km and a potassium-ion concentration of 3,200 ppm. Their finding further supports the assertion that the transformation of smectite to illite is not possible by over-pumping of groundwater at ambient temperature (25°C) and in the shallow aquifer system (300 m) of the Chou-Shui River alluvial fan.

Conclusion

This study adopted the novel smectite dehydration model to quantify the subsidence of land due to smectite dehydration in the Chou-Shui River alluvial fan and the Yun Lin offshore industrial infrastructure complex. The smectite dehydration model includes a model of the "hydration state of smectite", and a "solid solution model of smectite dehydration", incorporating a thermodynamic solid solution model and laboratory results concerning clay-water systems of swelling pressure, hydration state and basal spacing in the smectite interlayer. The amount of land subsidence attributed to smectite dehydration is determined using in-situ stratigraphic data collected from the land subsidence monitoring well, the model of the hydration state of smectite and the solid solution model of smectite dehydration.

The computed results for subsidence due to smectite dehydration caused by the over-pumping of groundwater in Shi-Kong (0–300 m), Mai-Liao (0–300 m), Tai-Shi (0–300 m) and Yi-Wu (0–200 m) are 23.23, 20.98, 19.88 and 17.97 cm, respectively, representing 12.56, 22.80, 9.56 and 9.45% of the accumulated subsidence measured in the field. The major land subsidence caused by smectite dehydration occurs in a shallow formation with a depth of 0–60 m, whereas only a small amount of subsidence developed in a deeper formation (>60 m).

The subsidence in the Yun Lin offshore industrial infrastructure complex at a depth of 200 m, calculated using Terzaghi's compaction theory for primary consolidation at 2.5 years, stabilizes and reaches its final accumulated value of 69.40 cm. However, the measured subsidence does not stabilize after 5 years. The difference between the measured and computed land subsidence is 32.75 cm, and is close to the 30.07 cm of subsidence including the dehydration of smectite. Thus, the inclusion of the effect of smectite dehydration yields a computed result that agrees with the field measurement. This study reveals that smectite dehydration is of importance in assessing and predicting land subsidence in shallow aquifer systems. It is also a valuable finding concerning the application of the developed novel smectite dehydration theory.

Future works should address the kinetics of smectite dehydration, the development of the solid solution model for smectite dehydration as a function of pressure and temperature in a radionuclear waste disposal site in which the backfill materials include smectite as a barrier, and an analysis of smectite dehydration due to the rapidly changing formation stress during fault displacement or an earthquake.

Acknowledgements The authors are grateful to the National Science Council, Republic of China, for financially supporting this research under contract Nos. NSC-90-02313-B-002-022 and NSC-91-02313-B-002-294.

References

Anderson GM, Crerar DA (1993) Thermodynamics in geochemistry. Oxford University Press, New York, 588 pp

Audet DM, Fowler AC (1992) A mathematical model for compaction in sedimentary basins. Geophys J Int 110:577–590

Audet DM (1995) Mathematical modeling of gravitational compaction and clay dehydration in thick sediment layers. Geophys J Int 122:283–298

Bethke CM (1986) Inverse hydrologic analysis of the distribution and origin of gulf coast-type geopressured zone. J Geophys Res 91(B6):6535–6545

Biot MA (1941) General theory of three-dimensional consolidation. J Appl Phys 12:155–164

Biot MA (1955) Theory of elasticity and consolidation for a porous anisotropic solid. J Appl Phys 26:182–185

Bray HJ, Redfern SAT, Clark SM (1998) The kinetic of dehydration in Ca-montmorillonite: an in situ X-ray diffraction study. Mineral Mag 62(5):647–656

Brown KM, Ransom B (1996) Porosity corrections for smectite-rich sediments-impact on studies of compaction, fluid generation. Geology 24:843–846

Central Geological Survey (1999) Project of groundwater monitoring network in Taiwan during first stage—Research report of Chou-Shui River alluvial fan: Water Resources Bureau Report, Ministry of Economic Affairs, ROC, 130 pp

Colten-Bradley VA (1987) Role of pressure in smectite dehydration—effects on geopressure and smectite-to-illite transformation. Am Assoc Petrol Geol Bull 71(11):1414–1427

Elliott WC, Matisoff G (1996) Evaluation of kinetic models for the smectite to illite transformation. Clays Clay Minerals 44(1):77–87

Eslinger E, Highsmith P, Albers D, Demayo B (1979) Role of iron reduction in the conversion of smectite to illite in bentonites in the disturbed belt, Montana. Clays Clay Minerals 27(5):327–338

Fitts TG, Brown KM (1999) Stress-induced smectite dehydration: ramifications for patterns of freshening and fluid expulsion in the N. Barbados accretionary wedge. Earth Planet Sci Lett 172:179–197

Freed RL, Peacor DR (1989) Geopressured shale and sealing effect of smectite to illite transition. Am Assoc Petrol Geol Bull 73:1223–1232

Fu MH, Zhang ZZ, Low PF (1990) Changes in the properties of a montmorillonite-water system during the adsorption and desorption of water: hysteresis. Clays Clay Minerals 38(5):485–492

Hawkins RK, Egelstaff PA (1980) Interfacial water structure in montmorillonite from neutron diffraction experiments. Clays Clay Minerals 28(1):19–28

Industry Bureau (2000) Yun Lin offshore industrial infrastructure complex development project, part IV: land subsidence monitoring and analysis: Industry Bureau Report, Ministry of Economic Affairs, ROC, 130 pp

Johnson JW, Oelkers EH, Helgeson HC (1992) SUPCRT92: Software package for calculating the standard molal thermodynamic properties of minerals, gases, aqueous species, and reactions among them as functions of temperature and pressure. Comput Geosci 18:899–947

Keren R, Shainberg I (1975) Water vapor isotherm and heat of immersion of Na/Ca-monotmorillonite systems I: homoionic clay. Clays Clay Minerals 23:193–200

 DOI 10.1007/s10040-005-0459-0

Liu CW, Lin WS, Shang C, Liu SH (2001) The effect of clay dehydration on land subsidence in Yun-Lin coastal area, Taiwan. Environ Geol 40(4–5):518–527

Mitchell JK (1993) Fundamentals of soil behavior, 2nd edn. Wiley, New York, 437 pp

Oliphant JL, Low PF (1982) The relative partial specific enthalpy of water in montmorillesite water systems and its relation to the swelling of these systems. J Coll Interface Sci 89(2):366–373

Pearson MJ, Small JS (1988) Illite-smectite diagenesis and palaeotemperatures in northern North Sea Quaternary to Mesozoic shale sequences. Clay Minerals 23:109–132

Powers MC (1967) Fluid-release mechanism in compacting marine mudrocks and their importance in oil exploration. Am Assoc Petrol Geol Bull 51(7):1240–1254

Ransom B, Helgeson HC (1989) On the correlation of expandability with mineralogy and layering in mixed-later clays. Clay Clay Minerals 37(2):189–191

Ransom B, Helgeson HC (1994a) A chemical and thermodynamic model of aluminous dioctahedral 2:1 layer clay minerals in diagenetic processes: regular solution representation of interlayer dehydration in smectite. Am J Sci 294:449–484

Ransom B, Helgeson HC (1994b) Estimation of the standard molal heat capacities, entropies, and volumes of 2:1 clay minerals. Geochim Cosmochim Acta 58(21):4537–4547

Ransom B, Helgeson HC (1995) A chemical and thermodynamic model of aluminous dioctahedral 2:1 layer clay minerals in diagenetic processes: dehydration of diotahedral aluminous smectite as a function of temperature and depth in sedimentary basins. Am J Sci 295:245–281

Sato T, Watanabe T, Otsuka R (1992) Effects of layer charge location and energy change on expansion properties of dioctahedral smectites. Clays Clay Minerals 40:103–113

Taiwan Sugar Corporation (1997) Establishment and operational management of groundwater monitoring network: Water Resources Bureau, Ministry of Economic Affair, ROC, 660 pp

Terzaghi K (1943) Theoretical soil mechanics. Wiley, New York, 510 pp

Water Resources Bureau (1997) Land subsidence survey in the coastal area of Taiwan. Water Resources Bureau Report, Ministry of Economic Affairs, ROC, 230 pp

Water Resources Bureau (2001a) Land subsidence monitoring and analysis in Taiwan. Water Resources Bureau Report, Ministry of Economic Affairs, ROC, 900 pp

Water Resources Bureau (2001b) Analysis of the regional hydrogeological characteristics. Chou-Shui River alluvial fan: Water Resources Bureau Report, Ministry of Economic Affairs, ROC, 164 pp

Zhang ZZ, Low PF (1989) Relation between the heat of immersion and the initial water content of Li, Na and K-montmorillonite. J Coll Interf Sci 133(2):461–472

 DOI 10.1007/s10040-005-0459-0